Supporting Information

Corrosion Resistant Functional Diamond Coatings for Reliable Interfacing of Liquid Metal with Solid Metals

Stephan Handschuh-Wang[‡,1,3], Tao Wang[‡,2], Lifei Zhu[1,3], Yang Xu[2], Lei Huang[2], Tiansheng Gan[1,3], Yongbing Tang[,2], Xuechang Zhou[*,1,3]*

[1]College of Chemistry and Environmental Engineering, Shenzhen University, Shenzhen 518055, P. R. China

[2]Functional Thin Films Research Center, Shenzhen Institutes of Advanced Technology, Chinese Academy of Sciences, Shenzhen 518055, P. R. China

[3]Guangdong Laboratory of Artificial Intelligence and Digital Economy (SZ), Shenzhen 518055, P. R. China

*****Correspondence and requests for materials should be addressed to Y. B. Tang (tangyb@siat.ac.cn) and X. C. Z. (email: xczhou@szu.edu.cn).

Movies:

Movie S1: Droplet impact test of a LM droplet (release height 8 cm) on diamond coated Ti with hierarchical roughness.

Movie S2: Droplet impact test of a LM droplet (release height 8 cm) on BDD coated Ti.

Movie S3: Application of the diamond coated Ti in a thermal management system. The upper diamond coated Ti sample was heated with a red laser while a video of the UV irradiation was captured. Here, the applied compression force was 6.8 N.

Movie S4: Application of the diamond coated Ti in a thermal management system. The upper diamond coated Ti sample was heated with a red laser while a video of the UV irradiation was captured. Here, the applied compression force was 0.45 N.

Synthesis of the diamond coatings:

Pretreatment of the titanium alloy (Ti6Al4V): The substrates were cut into sampled of 1 cm x 1 cm. Then, these substrates were grinded with 800, 1500 and 2000 (ISO/FEPA Grit designation) SiC sandpaper, successively. Afterwards, the substrates were cleaned in water and ethanol by ultrasonication for 10 min, successively.

Pretreatment of the n-type single crystalline (100) silicon: The substrates were mirror polished and cleaned by immersing in a cleaning solution, comprising 10 mL 32% H_2O_2 + 10 mL ammonia solution (25% - 28%) + 50 mL H_2O, for 10 min at 82 °C. Afterwards, the samples were cleaned in water and ethanol by ultrasonication for 10 min, successively.

Synthesis of flat nanocrystalline diamond coating: After pretreatment, the substrates, either titanium or silicon, were immersed in seeding solution, which affords high seeding density, and seeded ultrasonically for 15. The seeding solution was prepared as follows: Commercially available DND (*Chengdu*) particles dispersed in aqueous solution were employed as diamond seeds for nucleation and growth via HFCVD. To this base seeding solution [2-(Methacryloyloxy)ethyl]trimethylammonium chloride (TMAEMC, 75 wt.% in H_2O), reaching a final concentration of 5×10^{-6} mol/l and a final DND concentration of 0.005 wt.%. Furthermore, the pH was carefully adjusted to pH 3. Subsequently, the samples were placed into the HFCVD

chamber. During the deposition via HFCVD, the flow rates of the reaction gases CH_4 and H_2 were maintained at 32 sccm and 800 sccm, respectively, the temperature of the hot filaments was maintained at 2500 °C and the gas pressure was kept at 1.5 kPa. The deposition was performed for 20 min to generate flat nanocrystalline diamond coating.

Synthesis of structured diamond coating: After pre-treatment, the substrates were immersed in a diamond seeding solution, which affords low seeding density and controlled seeding. Commercially available detonation nanodiamond (DND) particles (*Plasmachem*) were employed to prepare this seeding solution. To the aqueous suspension of DNDs, DI water and oxalic acid was added to achieve a final concentration of 7×10^{-5} mol/L oxalic acid and 0.005 wt.% DND particles. The pH was carefully adjusted to pH 5. Subsequently, the samples were placed into the HFCVD chamber. During the deposition via HFCVD, the flow rates of the reaction gases CH_4 and H_2 were maintained at 32 sccm and 800 sccm, respectively, the temperature of the hot filaments was maintained at 2500 °C and the gas pressure was kept at 1.5 kPa. The deposition was performed for 1 h to synthesize well-distributed diamond hemispheres on the substrate. Subsequently, the procedure for obtaining flat nanocrystalline diamond coating was executed (pre-treatment (oxidation) and growth), resulting in a pinhole free diamond coating with a hierarchical roughness.

Synthesis of electric conductive boron doped diamond coating: For the synthesis of boron doped diamond (BDD) coating, the same seeding solutions as described before were utilized, corresponding to nanocrystalline flat BDD coating (4.2.2) and structured BBD coating (4.2.3). Furthermore, the synthesis of BDD coating via HFCV is similar to the diamond coatings described before. Briefly, BDD coating via HFCVD were generated by growth of BDD at the presence of the synthesis gases CH_4, H_2 and a mixture of 0.1% $(CH_3)_3B$ and 99.9% H_2 at flow rates of 32 sccm, 400 sccm and 160 sccm, respectively. The pressure during deposition was maintained at 2 kPa while the temperature of the hot filaments was maintained at 2500 °C. The deposition was executed for either 60 min for micro-sized crystallites and a rough surface or for 5 min for nano-sized crystallites. The rough discontinuous BDD coating was coated in a second coating step, comprising of seeding and HFCVD growth, similar to the structured diamond coating to achieve a continuous and pinhole free BDD coating, while the pinhole free nanocrystalline BDD coating can be used as received.

Evaluation of adhesion and corrosion resistance of the diamond coating: a) Friction test: The friction tests were carried out by a ball-on-disc tester. Si_3N_4 was used as counterpart balls with a diameter of 4 mm. The normal load was fixed to be 2 N. The sliding velocity was 150 r/min. The rotation diameter was 4 mm. The humidity was ca. 45% and the temperature was ca. 23 °C. b) adhesion test: The adhesion of the composite films was assessed by Rockwell C indentation tests with a load of 588 N.

Adhesion of diamond film:

The adhesion of the structured diamond coating on Ti was evaluated by Rockwell C indentation. In contrast, tape tests are typically too weak to delaminate hard coatings based on diamond. As for scratching test, these are not executed for diamond and other extremely hard coatings as in these experiments the measurement tip is easily damaged. Here, we show the Rockwell indentation test and a ball-on-disk sliding test. After indentation, no cracks or delamination was observed around the indentation impression, indicating good adhesion of the diamond coating on the Ti6Al4V alloy (see Figure S1a). Notably, this good adhesion is related to the bond formation between Ti and C during diamond deposition (i.e. 10.1016/j.jmst.2020.02.023). The friction test shows that after coating structured diamond on Ti, the friction coefficient decreased from 0.2 to 0.05 (see Figure S1b) and remains stable at this low friction coefficient after a first roll in process. Such ultralow friction coefficient combined with the stable friction coefficient indicates excellent wear-resistance of the diamond coating.

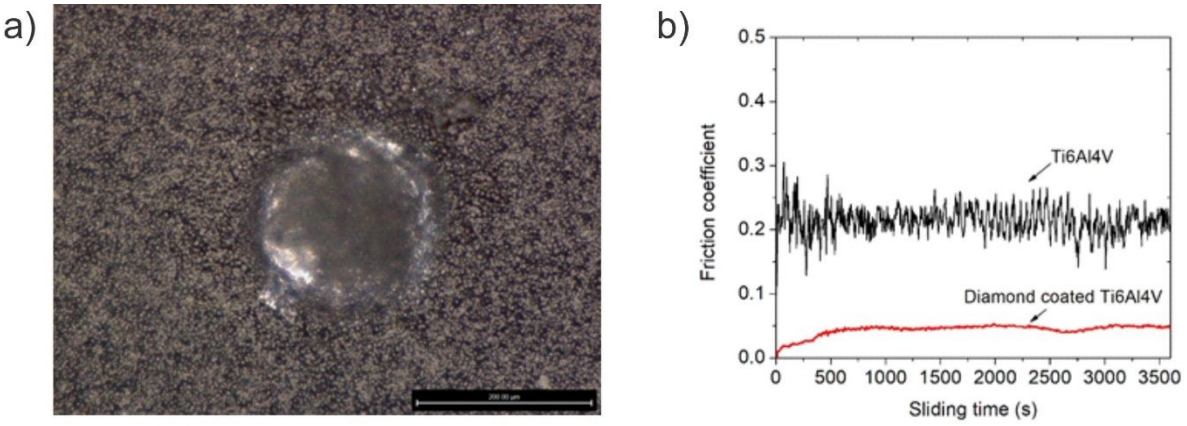

Figure S1. a) SEM micrograph of the structured diamond coating grown on Ti alloy after Rockwell C indentation with a load of 588N. b) Friction coefficient of Ti6Al4V alloy and hierarchical structured diamond coating on Ti with increasing sliding time.

Wettability of diamond coatings:

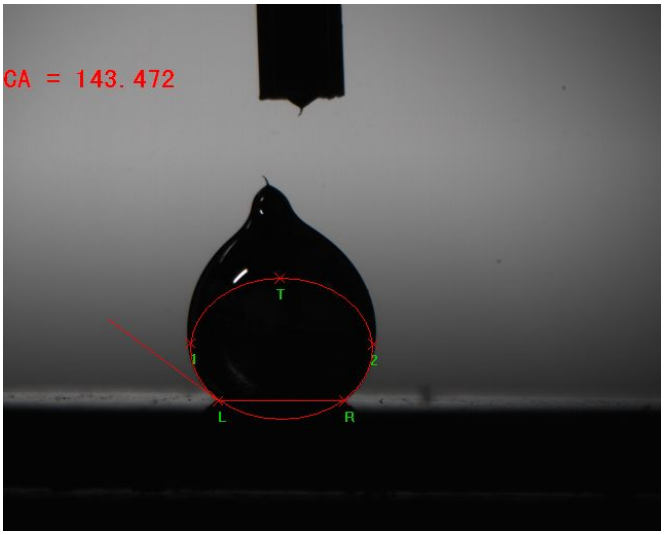

Figure S2 Contact angle of Galinstan on Ti alloy, showing a smaller contact angle than on the diamond coatings, presumably due to lower surface roughness than on the diamond coating.

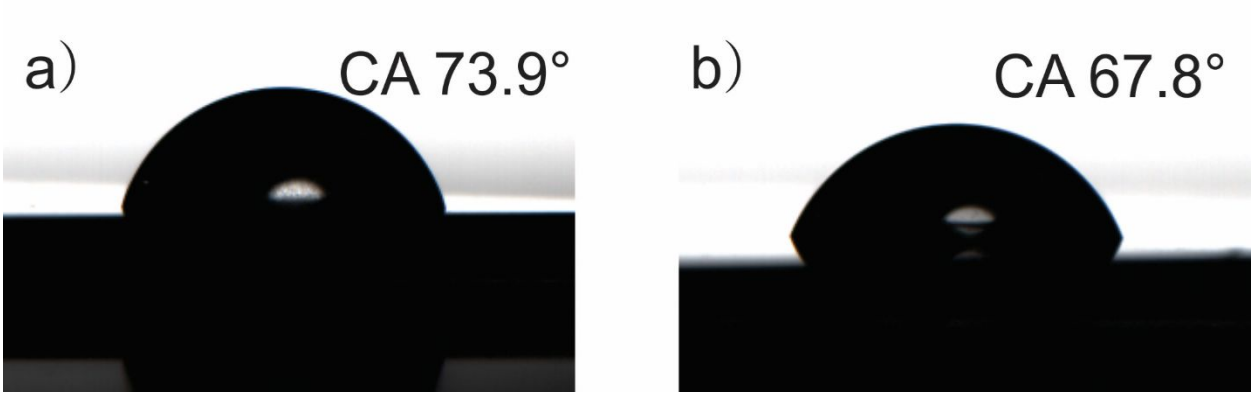

Figure S3. Water contact angle on flat (a) and structured (b) boron doped diamond coating on silicon substrate.

XPS analysis:

The XPS spectra in Figure S4 show the carbon peaks of BDD deposited on Si as well as structured diamond on Ti. The dominant peak at 284.3 eV denotes for the sp^3 C from the bulk, while the component at 285.15 eV is assigned to the CH_x with $x \geq 2$ on IIb crystals. Then, several small

components at higher energy can be detected, which denote for ether (286.4 eV), carbonyl (287.7 eV) and carboxylic (288.95 eV). The broadening at the base of the main peak toward lower energy can be ascribed to marginal contribution of sp^2 C (283 eV) (see also: 10.1002/pssa.200671123). Thus, surface oxidation of the BDD coating was detected, which can be ascribed to slow oxidation of the BDD by oxygen in air as it is stored (Electrochim. Acta, 2006, 51, 4612–4619). In contrast to this result, the carbon peak of structured undoped diamond on Ti only features the carbon sp3 C peak (283.8 eV) and the peak assigned to the CH_x with $x \geq 2$ on IIb crystals (284.4 eV). Here, no surface oxidation and no sp^2 species can be detected.

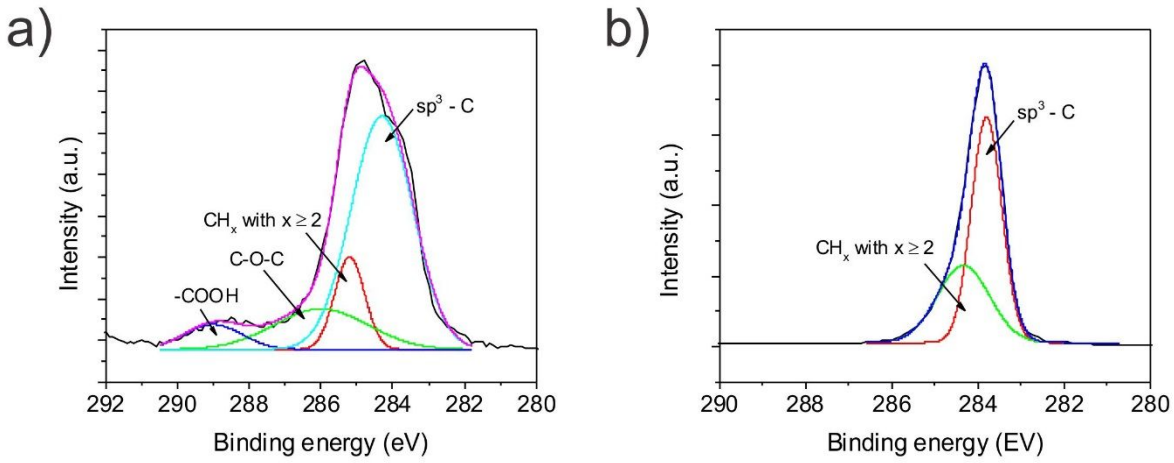

Figure S4: a) Part of the XPS spectra of BDD on Si, showing the carbon peak. b) Part of the XPS spectra of structured diamond coating on Ti, showing the carbon peak.

Table S1. Roll off angle of liquid metal droplets (Galinstan) on different substrates.

Substrate	**Roll off angle in °**	**Standard deviation in °**
Structured diamond coating on Si	12.8	3.6
Flat nanodiamond coating on Si	12.3	3.3
Flat BDD coating on Si	14.8	1.7
Structured BDD coating on Si	12.6	2.3
Structured diamond coating on Ti	8.5	1.1
Flat BDD coating on Ti	12.1	0.9

Cleaned silicon	26.0	3.9

Corrosion resistance of diamond coating:

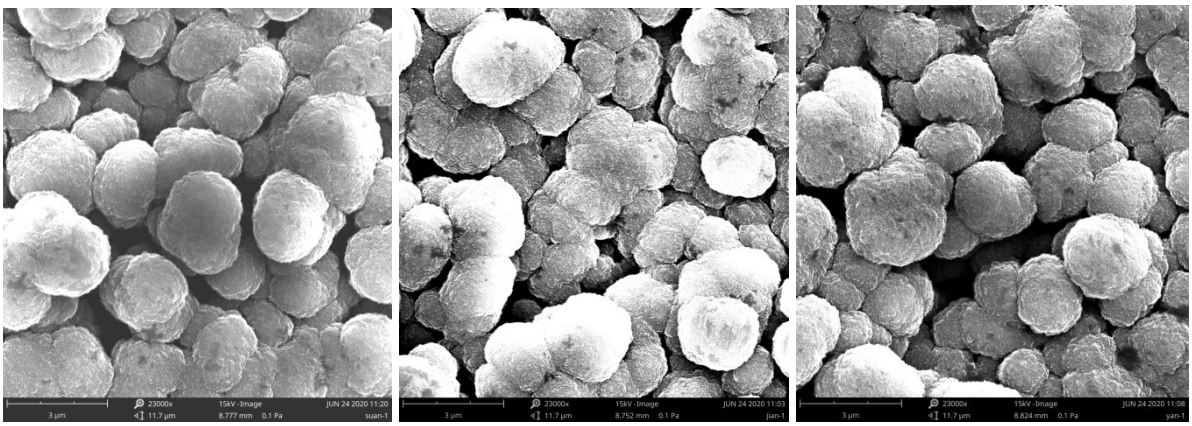

Figure S5. SEM surface morphology of structured diamond coating after immersion in 1mol/L HCl, 1 mol/L NaOH and 3.5 wt% NaCl for 7 days (from left to right), respectively.

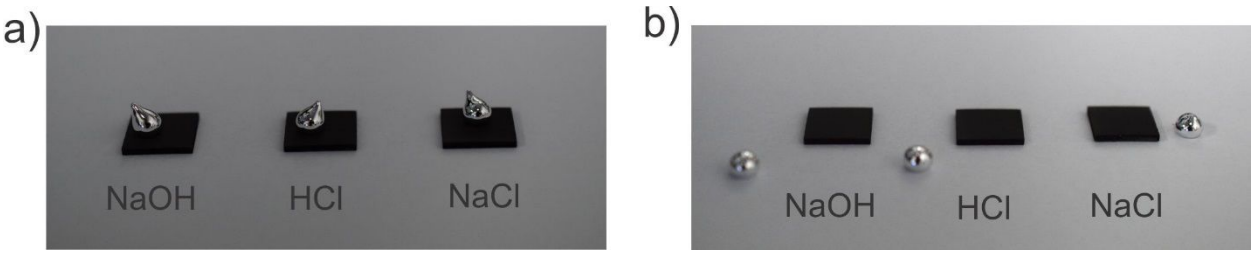

Figure S6: Liquid metal lyophobicity of structured diamond coating on Ti after treatment with 1 M NaOH, 1 M HCl and 3.5 wt% NaCl for 7 days. a) Liquid metal droplet deposited on the substrates. b) Substrates after removal of the liquid metal droplet by rolling them off.

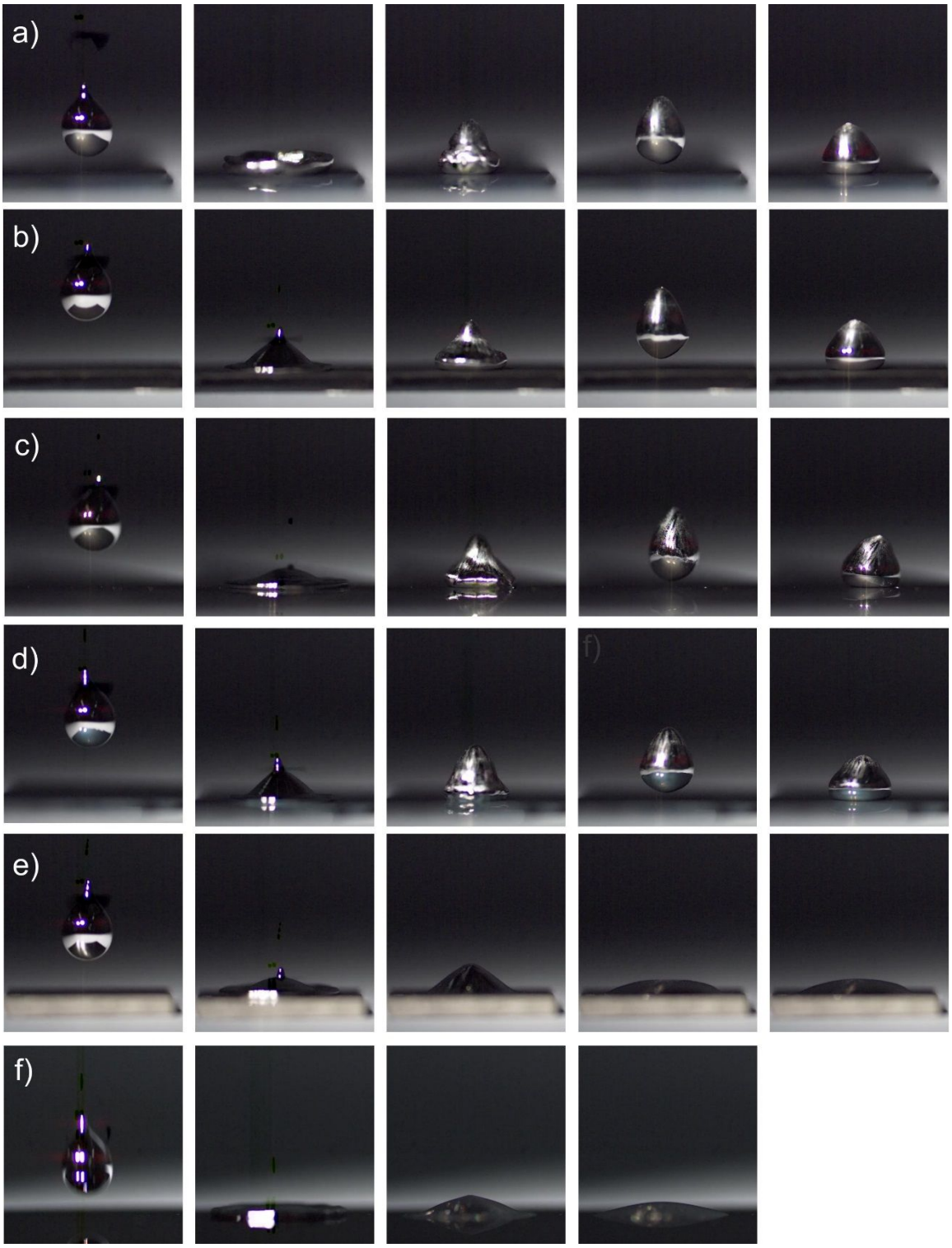

Figure S7. Droplet impact test of liquid metal on several substrates, that are rough diamond coating on silicon (a), flat diamond coating on Ti (b), rough boron doped diamond on silicon (c), flat diamond on silicon (d), polished titanium (e) and as-received silicon wafer (f). The release height of the 10 µL droplets was around 8 cm.

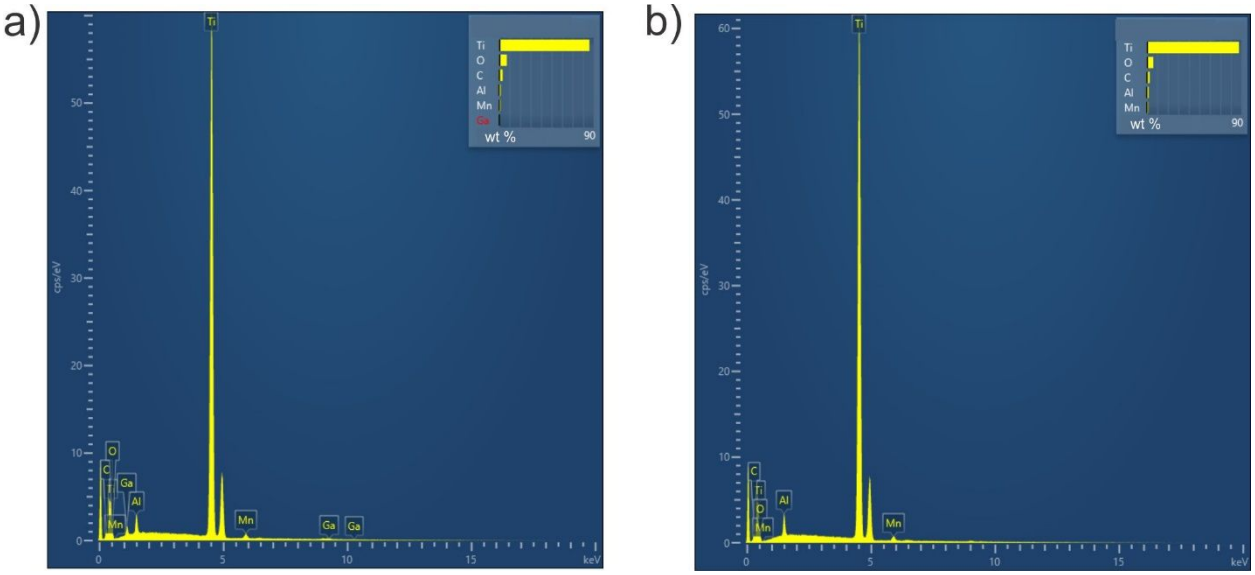

Figure S8 a) EDS spectra of titanium substrate after contact with Galinstan for 3 d and subsequent cleaning by rubbing with ethanol. b) EDS spectra of polished titanium (control).

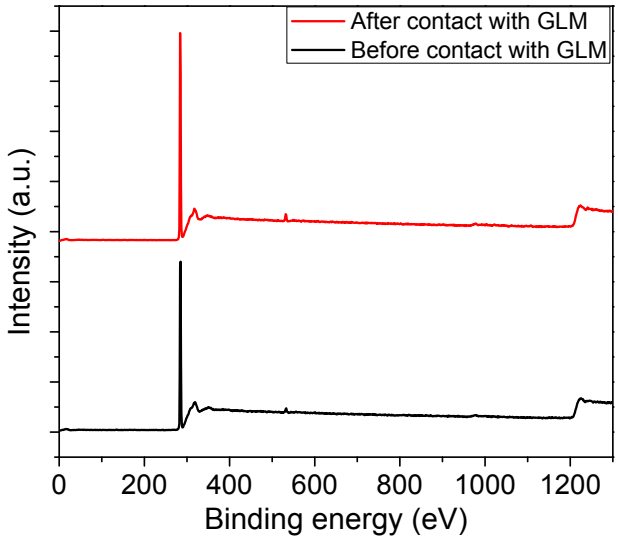

Figure S9. XPS spectra of structured diamond coating on Ti before and after contact with GLM for 3 weeks. No liquid metal peak (Ga/In/Sn) can be detected.

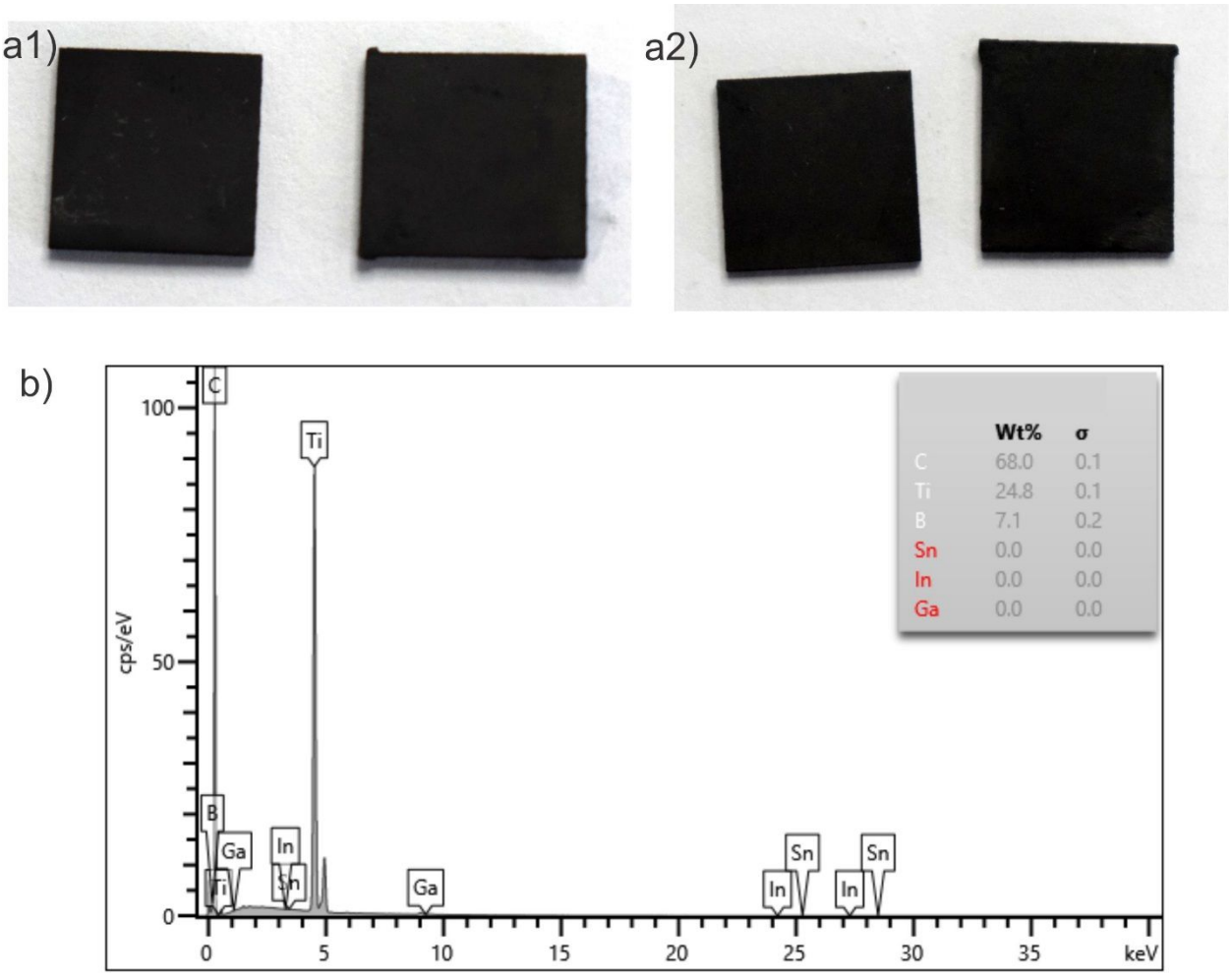

Figure S10. Photograph of BDD coated Ti samples after being in contact with liquid metal for 3 days during resistance measurement. Samples after cleaning with a1) ethanol and a2) 1 M HCl. b) EDS spectrum of the sample after cleaning with 1 M HCl.

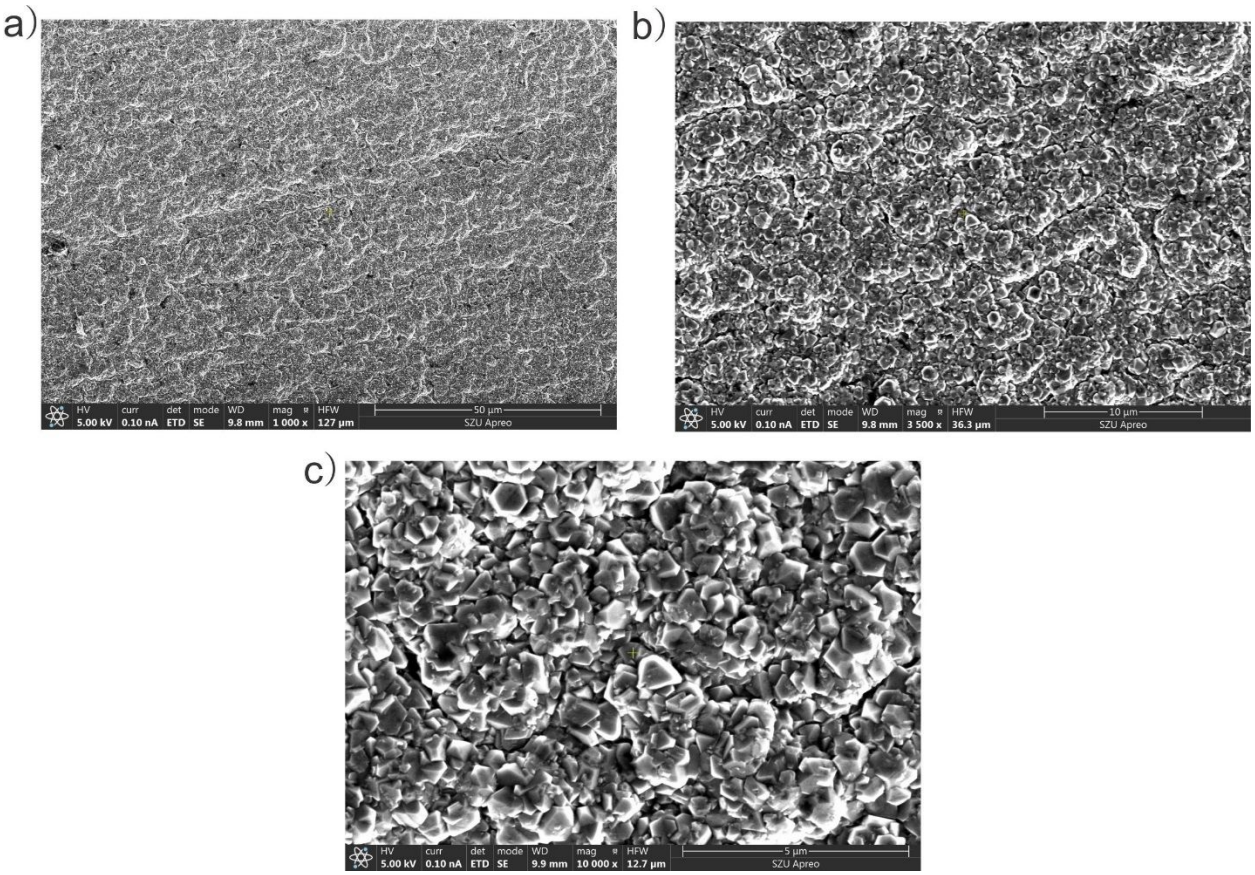

Figure S11 SEM micrographs of BDD coating on Ti after electric conductivity experiment and subsequent cleaning procedure. The coating was measured at (a) 1000x, (b) 3500x and (c) 10000x magnification.

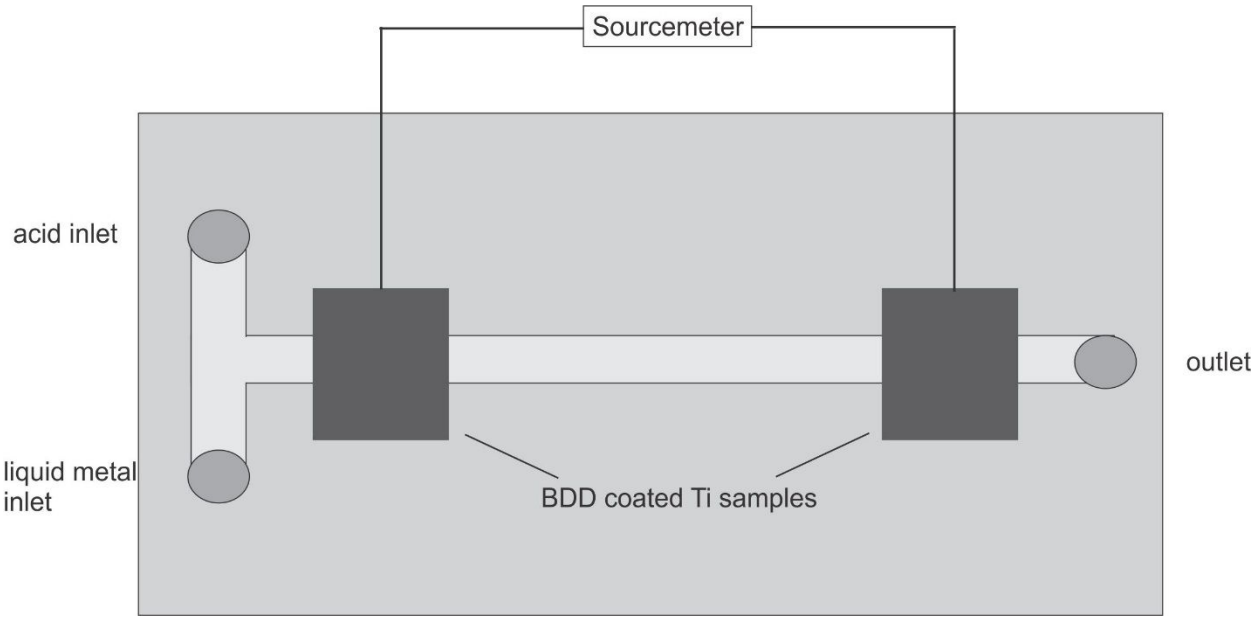

Scheme S1 Schematic illustration of the setup of the liquid metal enabled switch.